



Semi-interpenetrating network of polyethylene glycol and photocrosslinkable chitosan as an in-situ-forming nerve adhesive

Zohreh Amoozgar^{a,1}, Todd Rickett^{b,c,d,1}, Joonyoung Park^a, Chad Tuckek^c, Riyi Shi^{b,c,*}, Yoon Yeo^{a,b,*}

^a College of Pharmacy, Purdue University, 575 Stadium Mall Dr., West Lafayette, IN 47907, USA

^b Weldon School of Biomedical Engineering, Purdue University, 206 S. Martin Jischke Dr., West Lafayette, IN 47907, USA

^c Department of Basic Medical Sciences, Purdue University, 625 Harrison St., West Lafayette, IN 47907, USA

^d Indiana University School of Medicine, 340 W. 10th St., Indianapolis, IN 46202, USA

ARTICLE INFO

Article history:

Received 27 August 2011

Received in revised form 6 January 2012

Accepted 16 January 2012

Available online 25 January 2012

Keywords:

Chitosan

Polyethylene glycol

Semi-interpenetrating network

Nerve injury

Nerve adhesive

ABSTRACT

An ideal adhesive for anastomosis of severed peripheral nerves should tolerate strains imposed on rejoined nerves. We use blends of photocrosslinkable 4-azidobenzoic acid-modified chitosan (Az-C) and polyethylene glycol (PEG) as a new in-situ-forming bioadhesive for anastomosing and stabilizing the injured nerves. Cryo-scanning electron microscopy suggests that the polymer blends form a semi-interpenetrating network (semi-IPN), where PEG interpenetrates the Az-C network and reinforces it. Az-C/PEG semi-IPN gels have higher storage moduli than Az-C gel alone and fibrin glue. Nerves anastomosed with an Az-C/PEG gel tolerate a higher force than those with fibrin glue prior to failure. A series of ex vivo and in vitro cell experiments indicate the Az-C/PEG gels are compatible with nerve tissues and cells. In addition, Az-C/PEG gels release PEG over a prolonged period, providing sustained delivery of PEG, a potential aid for nerve cell preservation through membrane fusion. Az-C/PEG semi-IPN gels are promising bioadhesives for repairing severed peripheral nerves not only because of their improved mechanical properties but also because of their therapeutic potential and tissue compatibility.

© 2012 Acta Materialia Inc. Published by Elsevier Ltd. All rights reserved.

1. Introduction

Traumatic peripheral nerve injuries occur by blunt trauma and foreign object penetration, often resulting in complete or partial transection of the nerve [1,2]. These nerve injuries inflict significant economic and social burdens. The injured nerves are typically treated by surgical techniques, but the clinical outcome is not always satisfactory. Reportedly ~50% of the patients with nerve injuries showed good to excellent results or useful recovery after treatments, but 25–30% reported poor outcomes [3–6]. Therefore, an effective therapy of peripheral nerve injuries is eagerly awaited.

A standard procedure is to coapt the severed nerves by microsurgical suture [7]. A weakness of this technique, however, is that the suturing procedure involves multiple needle passages through the epineurium and results in structural disturbance in the nerves. Additionally, non-absorbable suture materials may cause foreign body reactions and scar tissue formation [8,9], which can interfere with the axonal regeneration and the nerve function after healing

[8,10]. Fibrin glue has been proposed as a potential replacement for sutures and has been welcomed as a simple and effective anastomosis technique [11–18]. However, the risk of disease transmission [19] and its weak mechanical strength [20] remain serious impediments to its use. Intense laboratory and clinical investigations have continuously improved the outcomes of nerve repair, but more effective methods to repair nerve injuries are still in high demand.

In an attempt to overcome some of the disadvantages of fibrin glue, we previously proposed a hydrogel based on photocrosslinkable chitosan (Az-C), prepared by partial conjugation of 4-azidobenzoic acid (ABA) to chitosan [21], as an alternative nerve adhesive [22,23]. Aqueous solution of Az-C forms a hydrogel upon ultraviolet (UV) illumination, which induces photolytic conversion of aryl azide to reactive nitrene, which undergoes ring expansion and reacts with the amines of Az-C to form an inter- and intramolecular chitosan network [22]. Chitosan hydrogel is an attractive substitute for fibrin glue or suture, due to its simplicity of application, tissue adhesiveness [24], safety and biocompatibility [25,26]. Our prior study showed that the Az-C gels were compatible with cultured neural cells and could reconnect nerves with mechanical properties comparable to fibrin glue [22]. However, further improvement in the mechanical strength would be desirable for the Az-C gels to provide reliable support for the anastomosed nerves during the critical healing period.

* Corresponding authors. Address: Weldon School of Biomedical Engineering, Purdue University, 206 S. Martin Jischke Dr., West Lafayette, IN 47907, USA. Tel.: +1 765 496 9608; fax: +1 765 494 6545 (Y. Yeo), tel.: +1 765 496 3018; fax: +1 765 494 7605 (R. Shi).

E-mail addresses: riyi@purdue.edu (R. Shi), yeyo@purdue.edu (Y. Yeo).

¹ Authors contributed equally.

In this study we aim to reinforce the Az-C network by adding a secondary polymer, polyethylene glycol (PEG). We prepared a composite hydrogel consisting of Az-C and PEG (Az-C/PEG gel) and investigated its mechanical and biological properties. The mechanical properties were investigated by rheological and tensile tests, and the biological effects of the gels were monitored using a neural cell culture model and electrophysiological experiments. We also envisioned the composite hydrogel as a local sustained delivery system of PEG, which has long been recognized as a potential membrane-fusing agent [27–29]. With this potential in mind, we examined the ability of Az-C gel to control PEG release.

2. Materials and methods

2.1. Materials

ABA was purchased from TCI America (Portland, OR, USA), and chitosan (15 kDa, deacetylation degree: 87%) from Polysciences (Warrington, PA, USA). PEG, 1-ethyl-3-[3-dimethylaminopropyl] carbodiimide (EDC), N,N,N',N'-tetramethylethylenediamine (TEMED), penicillin–streptomycin (Pen/Strep), nerve growth factor (NGF), ribonuclease A and a lactate dehydrogenase (LDH) assay were purchased from Sigma-Aldrich (St. Louis, MO, USA). Tube-A-Lyzer® (ready-to-use cellulose ester dialysis membrane) was purchased from Spectra/Por (Rancho Dominguez, CA, USA). Solvents were purchased from VWR (West Chester, PA, USA). WST-1 reagent (4-[3-(4-iodophenyl)-2-(4-nitrophenyl)-2H-5-tetrazolio]-1,3-benzene disulfonate) was purchased from Roche Applied Sciences (Indianapolis, IN, USA). TISSEEL® fibrin glue kit was obtained from Baxter Healthcare Corp. (Deerfield, IL, USA).

2.2. Synthesis of Az-C

Az-C gel precursor was synthesized as we described previously [22]. Briefly, TEMED (300 μ l, 1.98 mmol) was added to ABA (80 mg, 0.49 mmol) solution in 1 ml of dimethyl sulfoxide (DMSO), followed by the addition of 1 ml of aqueous solution of EDC (159 μ l, 0.9 mmol). The resulting mixture was vortex-mixed for 30 s and added to 200 ml of chitosan solution (2 mg ml⁻¹) in a 1:1 mixture of acidified water and DMSO. The reaction mixture was adjusted to pH 5 using 1 M hydrochloric acid. After overnight reaction at ambient temperature in darkness, the mixture was spun at 10,976 g for 3 h to remove the precipitated ABA. The ABA–chitosan conjugate (Az-C) remaining in the supernatant was purified by alkaline precipitation (pH 9.5) and redissolved in acidic solution (pH 3) at least five times. The final pH was adjusted to 5, and the Az-C was lyophilized and stored at –80 °C until use. Total salt content in dry mass was consistently found to be 8 wt.% [22]. Az-C was analyzed by photon nuclear magnetic resonance (¹H-NMR) spectroscopy (Bruker DRX500).

2.3. Preparation of Az-C and Az-C/PEG gels

Az-C was dissolved in 0.9% sodium chloride solution (saline) to 40 mg ml⁻¹. This precursor solution was gelled by illumination with a long-wavelength UV lamp (Black-Ray, UVP, radiation range 315–400 nm, peak at 365 nm). For preparation of Az-C/PEG gels, PEG was first dissolved in saline to 80 mg ml⁻¹, in which Az-C was added to 40 mg ml⁻¹. PEG was labeled according to the average molecular weight (as provided by the vendor) and the terminal functional group. For example, PEG with a molecular weight of 2000 Da and diol termini was labeled as P2k-dH; PEG (2000 Da) and monomethoxy terminus, P2k-mM; PEG (2000 Da) with dimethoxy termini, P2k-dM; PEG (4600 Da) with diol termini, P4.6k-dH; PEG (5000 Da) with monomethoxy terminus, P5k-mM; PEG

(6000 Da) with diol termini, P6k-dH; and PEG (8000 Da) with diol termini, P8k-dH.

2.4. Measurement of gelation time

Five or six drops (each 100 μ l) of the gel precursor solution were placed on a polyethylene dish and illuminated with the long-wavelength UV lamp at a distance of 6 cm. After UV illumination for 15, 20, 25, 30, 35, 40 or 45 s, the dish was removed to test the consistency of each drop. When the drop could be cleanly separated into two pieces by a plastic pipette tip passing along the diameter, the drop was considered to have formed a gel. Gelation time was defined as the time taken for all the drops to gel.

2.5. Mechanical analyses of hydrogels

The mechanical properties of the hydrogels were assessed with rheological analysis of the gels and tensile analysis of nerves anastomosed with the gels. These measurements were carried out at room temperature (~25 °C) for simplification of the study and comparisons with other studies [22,30,31], although values relevant to therapeutic applications remain to be measured at 37 °C.

2.5.1. Rheological analysis of hydrogels

Rheological properties of the gels were evaluated with a stress-controlled AR-2000 rheometer (TA Instruments, Leatherhead, Surrey, UK). To form an Az-C or Az-C/PEG gel, 450 μ l of precursor solution was put in a silicon sheet template (900 μ m thickness and 20 mm diameter) placed on a Peltier plate and illuminated with UV. A gel of this thickness is formed in less than 1 min, but the gels were illuminated for 10 min, simply to ensure the completion of gelation. A 20 mm parallel plate geometry was placed on the sample, maintaining a gap width of 900 μ m. A solvent trap filled with water was used to prevent the dehydration of the samples during the experiment. All measurements were performed at 25 °C. A stress sweep (σ , 0.07–1000 Pa) was performed at 0.1 Hz in a dynamic oscillatory mode to determine the storage modulus (G') of each gel. The G' value was calculated as a mean of all data points in the linear viscoelastic region.

2.5.2. Tensile analysis of nerve anastomosis

The efficacy of the hydrogels as nerve adhesives was tested *ex vivo* using an established protocol [22,32]. Animals were cared and handled according to a protocol (PACUC #04-049) approved by the Purdue Animal Care and Use Committee. Adult male Sprague-Dawley rats (Harlan Laboratories, Indianapolis, IN) were anesthetized by intramuscular injection of ketamine (80 mg kg⁻¹) and xylazine (10 mg kg⁻¹). Animals were euthanized by transcardial perfusion with cold, oxygenated Krebs's buffer solution, and sciatic nerves were removed from both legs. On a Teflon® surface (Dupont, Wilmington, DE, USA), nerve trunks were completely severed with a scalpel and apposed. A coating of ~100 μ l of either Az-C/P6k-dH or Az-C/P2k-dM was applied and UV illuminated for 60 s at 6 cm from the light source for crosslinking. Nerves were carefully lifted from the surface and inverted: an additional ~100 μ l coating was applied and gelled with an additional 60 s of UV exposure.

Using rubber grips, the anastomosed nerve was secured in a 100Q250 (Test Resources, Shakopee, MN, USA) computer-controlled vertical mechanical testing system. The unstressed length of the nerve was measured, and the force sensor tared to 0 N. At room temperature, nerves were stretched at 5 mm min⁻¹ (~0.1% strain s⁻¹) until failure, while the load cell recorded the system tension in real time. Data was exported to PC with Wincom® software (ADMET, Norwood, MA, USA).

Standard engineering definitions were used for data analysis. For example, strain (in%) was calculated as the change in nerve length divided by the length of the nerve prior to stretch. The maximum force value prior to failure was defined as the ultimate strength (in mN). Engineering stresses (in kPa) were estimated as the system tension divided by an average cross-sectional area for unstressed rat sciatic nerves (in mm²). We used 1.008 ± 0.083 mm² as the representative cross-sectional area, determined from sectioned sciatic nerves of comparably sized rats in our previous study [22]. This approximation was necessary because nerve measurement is complicated by the pliability of soft tissues. Stress–strain plots were generated, and the Young's modulus was calculated as the slope of the linear region of the characteristic curve.

2.6. Cryo-scanning electron microscopy (Cryo-SEM)

Solution (~50 µl) of Az-C, Az-C/P2k-dM or Az-C/P6k-dH was placed into a slit sample holder and crosslinked under UV. The sample holder was plunged into liquid nitrogen slush. A vacuum was created, and the sample was transferred to the Gatan Alto 2500 pre-chamber cooled to approximately –170 °C. The samples were fractured, sublimated for 10 min at –85 °C to remove unbound water and sputter-coated for 120 s with platinum. The samples were transferred to the microscope cryostage (–130 °C) for imaging. Samples were imaged with an FEI NOVA nanoSEM field emission scanning electron microscope using an Everhart–Thornley detector or a through-the-lens high-resolution detector. Parameters were 5 kV accelerating voltage, ~4–5 mm working distance, spot 3 and 30 µm aperture. Magnifications varied from $\times 1,000$ to $\times 40,000$, and images were displayed in a 30×26 cm format.

The average pore sizes were estimated from four randomly chosen images (two at $\times 5,000$ and two at $\times 10,000$) using Image J ver. 1.44n (NIH, Bethesda, MD). All the pores in the images were analyzed for Az-C and Az-C/P6k-dH. For Az-C/P2k-dM, pore size was determined for those in two arbitrarily defined fields (11.3 cm \times 7.5 cm) per image. Since the pores had irregular shapes, the pore size was defined as the longest length that could be drawn in each pore. Totals of 118, 110 and 304 pores were analyzed for Az-C, Az-C/P2k-dM and Az-C/P6k-dH, respectively, to determine the average pore size and size distribution.

2.7. Acute toxicological analysis

Sciatic nerves from male Sprague–Dawley rats were extracted as described in the previous section. The connective tissue surrounding the nerves was removed, and the isolated nerves were maintained in cold, oxygenated Krebs' buffer for at least 1 h. Nerves were placed in a double sucrose gap recording chamber with the stimulating and recording electrodes isolated with silicone grease. Stimulus was applied with a NeuroData® digital stimulator (Cygnus Technologies, Delaware Water Gap, PA, USA), while a bridge amplifier recorded the amplitude and latency of the elicited compound action potentials (CAPs). After conduction stabilized, CAPs were recorded for 10 min before the glue was applied. The fluid level was then lowered, and an 18-gauge syringe was used to completely coat the nerve surface with ~100 µl of Az-C/P2k-dM or Az-C/P6k-dH. UV light at a distance of 6 cm was maintained for 60 s to ensure gelation, and the fluid level was restored. A clear coating of Az-C/PEG gel was observed to surround the nerve following UV irradiation. Conduction through the nerve was allowed to briefly re-equilibrate before an additional 10 min CAP recording. For comparison between nerves from different animals, results from the post-exposure CAP amplitude and latency were normalized to the values prior to Az-C/PEG application.

2.8. Cytocompatibility studies

In standard 24-well flat-bottomed plates, ~100 µl of Az-C/P6k-dH or Az-C/P2k-dM gel precursor solution were spread on the bottoms of the wells. Solutions were gelled with 60 s of UV exposure at 6 cm. Rat PC-12 cells (American Type Culture Collection, Rockville, MD, USA) were plated at 20,000 cells per well on the Az-C/PEG gels or on the unmodified tissue culture polystyrene (TCPS). Cells were cultured in complete medium, consisting of 84% Dulbecco's modified Eagle's medium (DMEM), 12.5% horse serum, 2.5% fetal bovine serum, 1% Pen/Strep and 100 ng ml⁻¹ NGF at 37 °C in 5% CO₂ for 1, 4 or 7 days. Special care was taken to avoid removing loosely adherent cells when replacing the medium on alternating days. At the end of the culture periods, samples were incubated for 4 h in WST-1 reagent at 10% of the medium volume. Absorbance was measured on a VMax® kinetic microplate reader (Molecular Devices, Sunnyvale, CA, USA) at 450 nm, subtracting background absorbance at 650 nm.

In a separate analysis, the concentration of LDH in the culture medium was assessed spectrophotometrically using the standard protocol (TOX7) provided by the manufacturer. Briefly, cells were cultured with Az-C/PEGs, but low-serum medium was used to improve assay sensitivity. On days 1, 4, and 7, half the volume of cell medium was removed, and wells were refilled with serum-free medium (99% DMEM, 1% Pen/Strep, 100 ng ml⁻¹ NGF) and returned to the incubator. In a 96-well plate, 50 µl of the medium removed from culture was mixed with 100 µl of LDH assay mixture, as were 50 µl samples of untreated serum-free medium never exposed to cells (negative control). The reaction proceeded for 25 min at room temperature in darkness. Then 15 µl of 1 N HCl was added to each well to stop the reaction and the absorbance was measured at 490 nm, with the background absorbance at 650 nm subtracted.

To assess the affinity of the neural cells for the Az-C/PEG gels, the length of processes extended by cells growing on the gels was monitored. Cells were cultured in complete medium. On days 1, 4 and 7, 4% paraformaldehyde was used to fix the cultures, 0.1% Triton X-100 to permeabilize the cell membranes and 10 µg ml⁻¹ RNase to remove any non-nuclear amino acids. Cell nuclei were stained with propidium iodide at 0.05 mg ml⁻¹, and cytoskeletal actin was stained by AlexaFluor-488-conjugated phalloidin at 165 nM. After 25 min, wells were washed with PBS and imaged. For each sample type, four photomicrographs were acquired at random locations within each of our wells, for a total of 16 images per time point. A Nikon Diaphot 300 fluorescent microscope with a Diagnostic Instruments 11.2 color mosaic CCD camera was used to image cells, and the recorded images were analyzed using Image-Pro® software (MediaCybernetics Inc., Bethesda, MD, USA). Cell processes were measured with ImageJ (NIH, Bethesda, MA, USA). All visible neurites were measured unless they touched other cells or extended beyond the image boundary. Only the longest process of branching neurites was measured. Process lengths were averaged for each well, and the wells were pooled to produce mean extension values ($n = 4$ for each surface and time point).

2.9. PEG release kinetics

P2k-dM release from Az-C/P2k-dM gel was observed in vitro. The gel was formed in a dialysis tube to prevent breakage of the gel, which would change its surface area and complicate the sampling. To examine the direct effect of the dialysis membrane on P2k-dM release, P2k-dM solution was put in the tube and tested identically in parallel. Briefly, 1 ml of Az-C/P2k-dM gel precursor solution or P2k-dM solution (80 mg ml⁻¹) was placed in a Tube-A-Lyzer® dialysis tube (MWCO: 8–10 kDa) and put under a UV lamp without a cap. It was illuminated for 10 min – much longer

than the determined gelation time (<1 min) – to ensure complete gelation. After gel formation, the tube was closed, then placed in 40 ml of phosphate-buffered saline (PBS; 10 mM phosphate, 137 mM NaCl, pH 7.4) and incubated at 37 °C with constant agitation. At pre-determined time points, the release medium was replaced with fresh PBS and the sampled medium was stored at 4 °C until analysis. PEG concentration in the medium was measured using high pressure liquid chromatography (HPLC 1100 series, Agilent Technologies, Palo Alto, CA) and a series of gel permeation chromatography (GPC) columns (all 7.8 × 300 mm) consisting of Ultrahydrogel™ 250, Ultrahydrogel™ 500 and Ultrahydrogel™ 1000. PBS was used as an eluent and flowed at 1 ml min⁻¹. PEG was detected using a refractive index detector.

2.10. Statistical analysis

All data were expressed as averages with standard deviations. Analysis of variance was used to determine statistical differences among the groups, and multiple contrasts were performed with the Tukey test unless stated otherwise. A *p*-value of <0.05 was considered statistically significant.

3. Results

3.1. Synthesis of Az-C and preparation of hydrogels

Conjugation of ABA to chitosan was confirmed by ¹H-NMR: chitosan: 2.01 (s), 3.0 (s, broad), 3.2–4 (m); 4-azidobenzamide: 7.17–7.19 (d, *J* = 10 Hz), 7.81–7.83 (d, *J* = 10 Hz). According to comparison of an integrated area of peaks in 7–8 ppm (4H, benzene) and that in 3–4 ppm (6H, chitosan), ~2% of amino groups in chitosan were conjugated with ABA and converted to 4-azidobenzamide.

Precursor solutions prepared with Az-C or blends of Az-C and various PEGs formed soft gels in <1 min under UV illumination (Table 1). A 40 mg ml⁻¹ Az-C solution gelled in less than 40 s. Most Az-C/PEG solutions gelled relatively quickly (in 20–25 s), except for the Az-C/P2k-dH, which took 40–45 s to gel.

3.2. Rheological analysis (Fig. 1)

Az-C gel (40 mg ml⁻¹) showed a constant storage modulus (*G'*) of 877.1 ± 122.5 Pa, whereas fibrin glue showed a *G'* of 53 ± 20.6 Pa (*p* < 0.001 vs. Az-C) [22]. Az-C was distinguished from fibrin glue not only in *G'* but also in the tolerated stress range (i.e. the linear viscoelastic region) (Supporting Fig. 1). Incorporation of 80 mg ml⁻¹ P6k-dH increased the *G'* of gel by 1.7 folds (*p* < 0.05 vs. Az-C). P4.6k-dH and P8k-dH had similar effects, but statistical differences were not observed due to the large variation of data. Interestingly, the same level of P2k-dH slightly decreased the *G'* of the gel, although the difference was not statistically significant (*p* = 0.92). Hydrogels that gelled faster had relatively high *G'* values.

To test if the hydroxyl groups in PEG played a role in the hydrogel formation, P2k-dH and P6k-dH were replaced with PEGs that

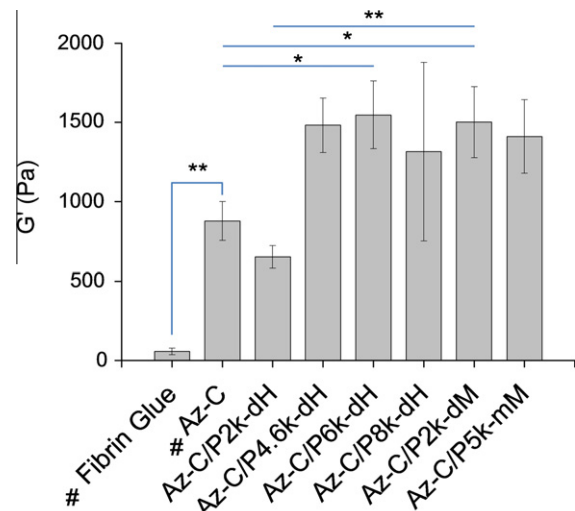


Fig. 1. Storage moduli (*G'*, Pa) of different hydrogels. The *G'* value was calculated as the mean of all data points in the linear viscoelastic region. The graph shows average *G'* values and standard deviations of 3–6 independently and identically prepared samples: fibrin glue (*n* = 6); Az-C (*n* = 4); Az-C/P2k-dH (*n* = 3); Az-C/P4.6k-dH (*n* = 3); Az-C/P6k-dH (*n* = 4); Az-C/P8k-dH (*n* = 3); Az-C/P2k-dM (*n* = 4); and Az-C/P5k-mM (*n* = 3). #Data from our previous study [22]. **p* < 0.05; ***p* < 0.01.

had comparable molecular weights but a methoxy group in at least one terminus (P2k-dM and P5k-mM, respectively). Contrary to Az-C/P2k-dH (*G'*: 650.5 ± 71.7 Pa), Az-C/P2k-dM had a *G'* value of 1501.1 ± 224.7 Pa, 1.7-fold higher than that of the Az-C gel (*p* < 0.05) and comparable to that of Az-C/P6k-dH. The replacement of P6k-dH with P5k-mM did not make significant difference (*p* = 0.15). Since Az-C/P2k-dM and Az-C/P6k-dH significantly outperformed Az-C in the rheological analysis, the two gels were used as representative Az-C/PEG gels in subsequent studies.

3.3. Tensile analysis of nerve anastomosis

The ability of nerves anastomosed with gels to tolerate longitudinal tensions was evaluated by tensile analysis. Az-C/P2k-dM and Az-C/P6k-dH gels were tested under the same condition as in our previous work [22], and their tensile strengths were compared with the reported values of Az-C and fibrin glue. In contrast to the nerves joined by fibrin glue, which tolerated 69.5 ± 31.6 mN (*n* = 8) before failure [22], those anastomosed by Az-C/P2k-dM and Az-C/P6k-dH withstood 108.2 ± 31.8 mN (*n* = 8) and 92.2 ± 14.7 mN (*n* = 9), respectively (Fig. 2A). Az-C/P2k-dM performed significantly better than fibrin glue (*p* = 0.019), but the difference between Az-C/P6k-dH and fibrin glue was not found to be significant (*p* = 0.225). The differences in tensile strength among Az-C, Az-C/P2k-dM and Az-C/P6k-dH were not statistically significant. Upon failure, Az-C/PEG gels separated within the gel, leaving the gel residue on both nerve trunks, similar to Az-C [22]. In contrast, strain on fibrin-anastomosed nerves resulted in separation of the nerves from the adhesive. According to the strain at failure values, all gels tolerated a similar degree of stretch: fibrin glue, 19.2 ± 12.7% [22]; Az-C, 15.0 ± 4.1% [22]; Az-C/P2k-dM, 21.4 ± 7.3%; and Az-C/P6k-dH, 19.6 ± 3.3% (Fig. 2B).

The engineering stresses of the anastomosed nerves were estimated to be 107.4 ± 31.6 kPa for Az-C/P2k-dM and 91.5 ± 15.6 kPa for Az-C/P6k-dH. The former was significantly improved as compared to the stress tolerated by fibrin glue (68.9 ± 31.4 kPa) [22]. Estimated from the representational stress–strain curves, the mean Young's moduli for the anastomosed nerves were 960 ± 305, 766 ± 71 and 528 ± 247 kPa for Az-C/P2k-dM, Az-C/P6k-dH and fibrin glue, respectively. The nerves anastomosed by Az-C/P2k-dM

Table 1
Concentration of hydroxyl groups in each gel and the gelation time.

Gel precursors	Hydroxyl end functional group (mM) present in each gel	Gelation time (s)
Az-C	Not applicable	38.5 ± 2.4 (<i>n</i> = 10)
Az-C/P2k-dH	0.08	43.5 ± 2.4 (<i>n</i> = 10)
Az-C/P4.6k-dH	0.035	23.8 ± 2.3 (<i>n</i> = 8)
Az-C/P6k-dH	0.027	22.1 ± 2.7 (<i>n</i> = 6)
Az-C/P8k-dH	0.02	23.8 ± 2.3 (<i>n</i> = 8)
Az-C/P2k-dM	0	22.0 ± 2.7 (<i>n</i> = 5)
Az-C/P5k-mM	0.016	23.3 ± 2.6 (<i>n</i> = 6)

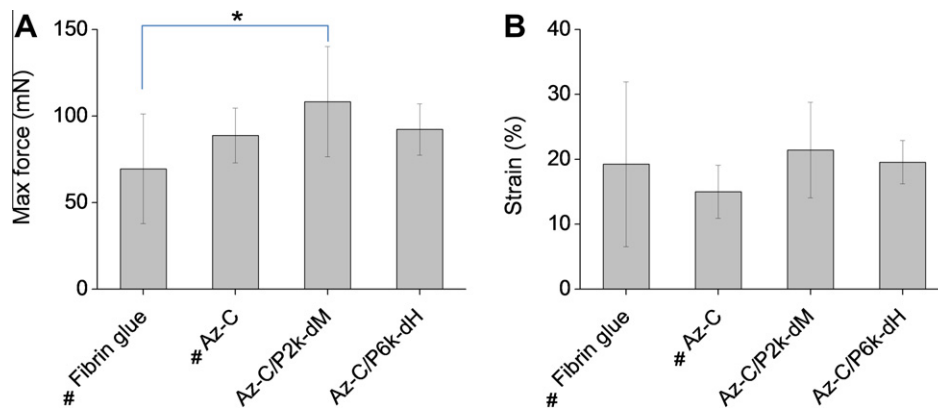


Fig. 2. (A) Maximum tolerated force and (B) strain at failure for severed peripheral nerves anastomosed with fibrin glue ($n = 8$), Az-C ($n = 8$), Az-C/P2k-dM ($n = 8$) and Az-C/P6k-dH ($n = 9$). #Data from our previous study [22]. * $p < 0.05$.

gels were significantly stiffer than those anastomosed by fibrin glue ($p = 0.003$), while the values for Az-C/P6k-dH and fibrin glue were not significantly different ($p = 0.098$).

3.4. Hydrogel characterization by cryo-SEM

To evaluate structural difference between Az-C and Az-C/PEG gels, selected gels were observed using cryo-SEM. Since samples are rapidly cooled to vitrify water in cryo-SEM, the samples can avoid structural changes due to crystallization of water. Sublimation of unbound or loosely bound water revealed “pores” surrounded by hydrogel frameworks (“cells”) that consisted of solid components of gels (Az-C and PEGs) and bound water. Notably, Az-C/PEG gels did not sublime well on the initial attempt and needed to be re-dried. This indicates that the Az-C/PEG gels had a higher affinity for unbound water than the Az-C gel. As shown in Fig. 3, Az-C and Az-C/P2k-dM displayed relatively homogeneous pores, measuring 6.8 ± 1.7 and 1.7 ± 0.5 μm , respectively. On the other hand, pores of Az-C/P6k-dH were heterogeneous, ranging widely, from 1 to 13 μm . At higher magnifications, all gels showed fibrous materials either anchored into the smooth wall of the cells (Az-C) or in the pores and as part of the cells (Az-C/P2k-dM, Az-C/P6k-dH) (Supporting Fig. 2). The fibrous materials appeared to be solid gel components deprived of the bound water.

3.5. Electrophysiology

The ability of axons to conduct an electrophysiological signal is highly dependent on the external milieu. Therefore, acute nerve impairments in response to new chemical species are often evaluated by observing electrophysiological signals of isolated peripheral nerves [33–35]. To evaluate potential toxicity of Az-C/PEG gels on nerves, their acute effect on CAP amplitude and latency was analyzed *ex vivo*, as described in our previous publications [22,23]. CAP amplitude is a measure of the relative number of axons conducting signal, and latency is defined as the delay between the nerve stimulation and the CAP recording. A one-tailed paired Student’s *t*-test was used to evaluate significance of changes in CAP amplitude and latency. Application of Az-C/PEG gels did not significantly affect CAP conduction through nerves (Fig. 4A). The CAP amplitude and latency for nerves coated with Az-C/P2k-dM ($n = 8$) were $102.6 \pm 15.3\%$ ($p = 0.44$) and $109.2 \pm 9.6\%$ ($p = 0.13$) of the average pre-exposure values, respectively. Similarly, CAP conduction was not significantly altered following the application of Az-C/P6k-dH ($n = 7$), with an amplitude only reduced inconsequentially (by $0.5 \pm 20.3\%$, $p = 0.48$) and a minor increase in latency of $12.7 \pm 18.7\%$ ($p = 0.15$). Time histories (Fig. 4B) showed regular

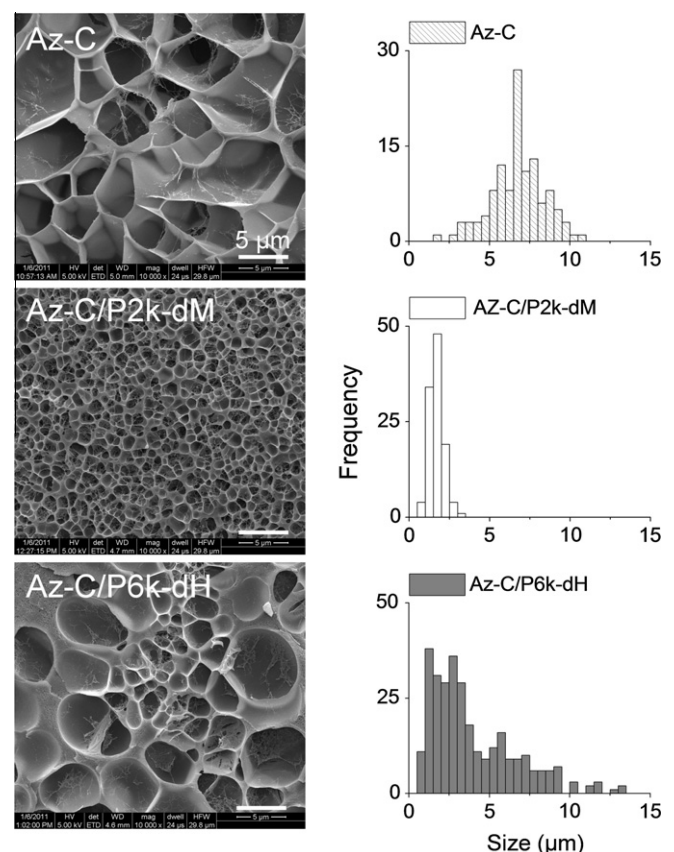


Fig. 3. Representative cryo-SEM images and pore size distribution of Az-C, Az-C/P2k-dM and Az-C/P6k-dH. Magnification: $\times 10,000$.

conduction before and after adhesive application, except for the periods when Az-C/PEG gel precursor solutions were applied and photocrosslinked.

3.6. Cytocompatibility

Potential cytotoxicity of Az-C/PEG gels was evaluated with the rat pheochromocytoma PC-12 cell line using the WST-1 cell proliferation assay and LDH cytotoxicity assay. PC-12 cells were chosen for the extensive use in studies of neuronal differentiation [36]. As measured by WST-1 metabolism, the viability of PC-12 cultures on the three surfaces was similar on days 1 and 4 (Fig. 5A). On day 7,

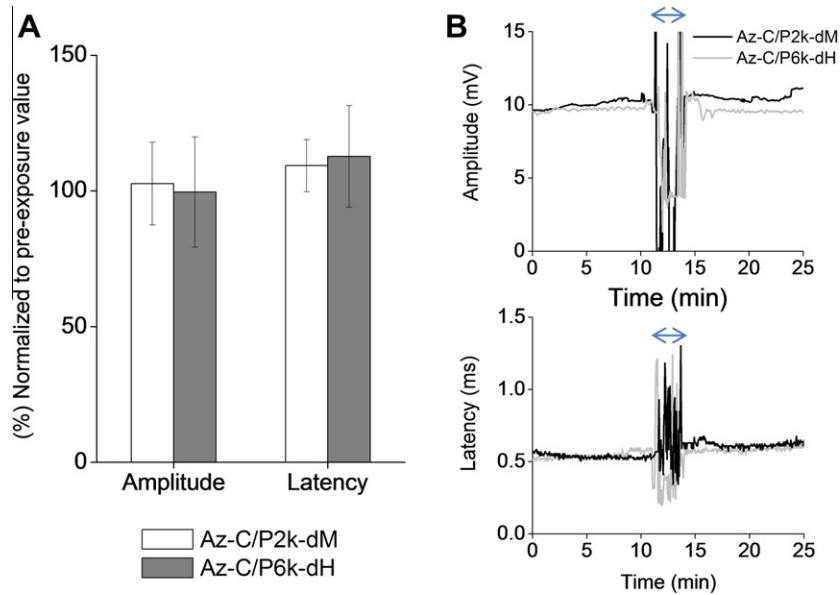


Fig. 4. (A) Mean CAP amplitude and latency after exposure to Az-C/P2k-dM and Az-C/P6k-dH gels, normalized to their values pre-exposure. (B) Representative time histories are shown for CAP amplitude and latency before, during and after the gel application. Double-headed arrows indicate the period when the fluid level was lowered for application of Az-C/PEG coating and photopolymerization. Upon refilling with Krebs's solution, the CAP amplitude and latency were restored to levels comparable to the previous values.

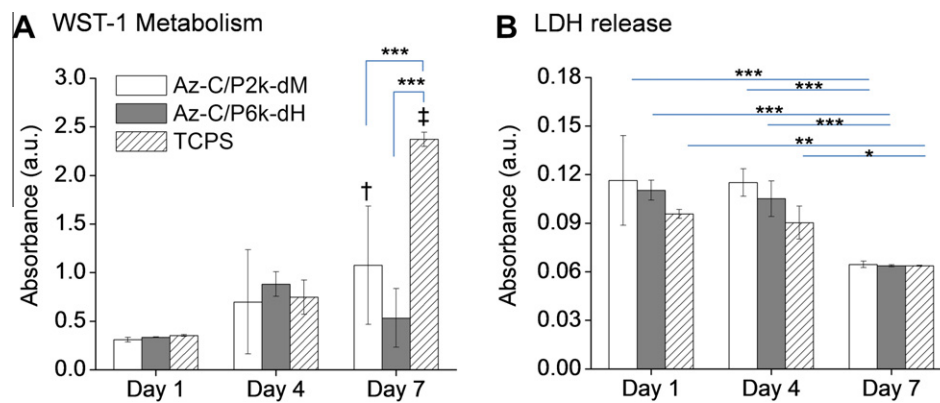


Fig. 5. Survival and viability of PC-12 cells cultured on surfaces of Az-C/P2k-dM, Az-C/P6k-dH and TCPS were assessed through (A) metabolism of WST-1 and (B) release of LDH. Spectroscopic absorbance readings were taken on days 1, 4 and 7, and values are expressed in arbitrary units. * $p < 0.05$; ** $p < 0.01$; *** $p < 0.001$; †significantly increased from day 1 ($†p < 0.05$; $††p < 0.001$).

cells growing on the TCPS metabolized significantly more tetrazolium salt than those on the Az-C/P2k-dM and Az-C/P6k-dH gels ($p < 0.0001$, $n = 4$ for all groups). No significant difference was observed between the two Az-C/PEG gels at any time point. Generally, tetrazolium salt metabolism increased with time, but significant differences were observed only between days 1 and 7 for Az-C/P2k-dM and TCPS. Measurements of LDH concentration in the culture medium (Fig. 5B) showed a similar trend in cellular response to the WST-1 assay in that performances of the groups were comparable on days 1 and 4. There were no significant differences in the LDH release among the PC-12 cells growing on different surfaces at any time point ($n = 4$ for all groups). LDH release decreased over time in all cases, with LDH levels on day 7 significantly lower than those on days 1 and 4.

PC-12 cell morphology was normal on all surfaces (Fig. 6A). Relatively few cells were observed to extend neurites on day 1. The number of cells possessing neurites increased with time. The mean process length for PC-12 cells growing on each surface is shown in Fig. 6B. Neurite lengths increased significantly from day 1 to day 4

for Az-C/P6k-dH and TCPS (both $p < 0.05$). On day 7, the cells on TCPS surfaces showed significantly longer processes ($63.8 \pm 19.7 \mu\text{m}$) than those on Az-C/P2k-dM ($36.8 \pm 6.0 \mu\text{m}$, $p = 0.015$) or Az-C/P6k-dH ($36.3 \pm 8.4 \mu\text{m}$, $p = 0.013$).

3.7. PEG release from Az-C/PEG gels

To examine the ability of Az-C gel to control the temporal availability of PEG applied in the nerves, PEG release was monitored over 25 days using the Az-C gel containing P2k-dM, which was considered to be the optimal composite gel of the tested gels. The Az-C gel attenuated the release of P2k-dM to a greater extent than that owing to the dialysis membrane. While $86.5 \pm 24.9\%$ of total PEG was released from the dialysis tube by day 2, $42.3 \pm 3.3\%$ of total PEG was released from Az-C/P2k-dM during the same period, followed by slow release of the remaining over the next 23 days (Fig. 7). The first $\sim 60\%$ release was best fitted by the power law [37] $M_t/M_\infty = Kt^n$, where M_t is the cumulative PEG mass released up to each time point, M_∞ is the maximum possible

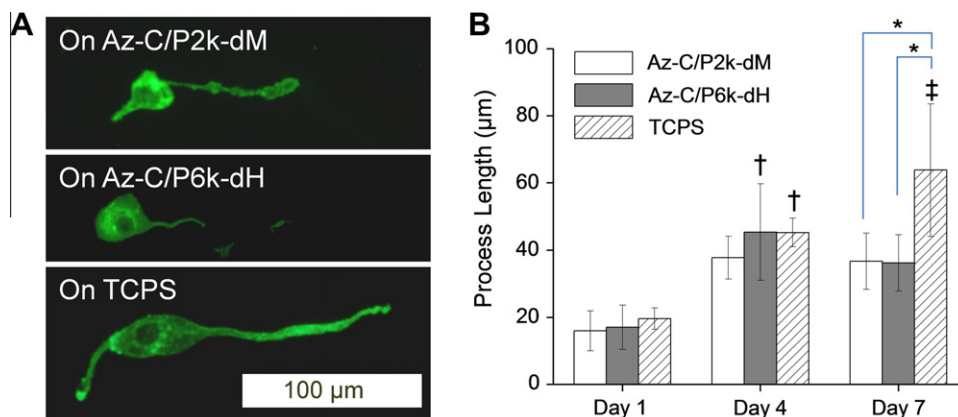


Fig. 6. (A) Representative photomicrographs of PC-12 cells after 7 days of growth on surfaces of Az-C/P2k-dM, Az-C/P6k-dH and TCPS. (B) Mean length of processes extended by these cells on days 1, 4, and 7. * $p < 0.05$; †significantly increased from day 1 († $p < 0.05$; ‡ $p < 0.001$).

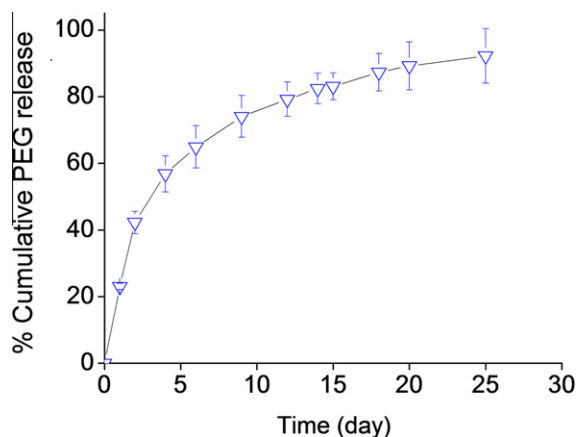


Fig. 7. In vitro release kinetics of P2k-dM from Az-C/P2k-dM gel. Data are expressed as averages with standard deviations of three identically and independently prepared samples.

cumulative drug release and K is the release constant. The release exponent (n) was 0.45, which, given the cylindrical geometry, indicated that the PEG release followed Fickian diffusion.

4. Discussion

A crucial element of peripheral nerve healing is the formation of the fibrin matrix between the nerve stumps followed by the re-establishment of connective tissue. The exact time course of nerve healing is not known, but it has been shown that regenerating nerves regain a significant portion of their strength within the first week of anastomosis [38,39]. Therefore, we aimed to achieve a bioadhesive that could stabilize the coated nerves for at least 1 week. For this purpose, we proposed to use Az-C gel [22], which could be applied as a viscous liquid that flows around the damaged nerves temporarily held together. The gel precursor solution could be quickly crosslinked in situ by short-term UV illumination, covering the tubular part of the nerves and providing a reliable linkage during the healing process. While Az-C has many advantages, such as bioadhesive properties, in situ crosslinkability and the lack of significant toxicity or potential for disease transmission, the gel should be further improved to better tolerate longitudinal or shear strain and provide a reliable support for the rejoined nerves until the restoration of anatomical continuity. While it is conceivable

to increase the crosslinking density by increasing the ABA conjugation, additional ABA decreases the aqueous solubility of the Az-C and complicates its application (data not shown). This solubility limitation was recognized by Ono et al. and partly addressed by modification with lactobionate, but the Az-C lactobionate gel (50 mg ml^{-1}) was not superior to fibrin glue in binding strength [24].

In this study we show that simple blending of PEG improves the mechanical properties of the gel, as assessed by rheological and tensile analyses. The increased storage modulus G' (except for Az-C/P2k-dH) is attributable to the formation of a semi-interpenetrating polymer network (semi-IPN) between Az-C and PEG. A semi-IPN is a polymer network formed by polymerization or crosslinking of one polymer (in our case, Az-C) in the presence of the other (PEG) [40], where the former forms a covalent network and the latter physically entangles with the former and reinforces the network [41]. Semi-IPN has been mainly used to improve the mechanical properties of a gel [42,43], but it is also used to provide additional functionalities, such as cell adhesiveness [44] or drug diffusion barrier [45]. In the present case, Az-C/PEG semi-IPNs showed higher mechanical strength than networks made of Az-C alone, due to the cooperation of covalent and physical interactions. Moreover, the relatively short gelation time of Az-C/PEG mixtures suggests that PEG may also have provided a microdomain where the reactive groups of Az-C are concentrated and undergo covalent crosslinking more rapidly. Cryo-SEM images of selected Az-C/PEG gels show the structure of Az-C/PEG semi-IPNs. The addition of P2k-dM to Az-C gel precursor significantly increased the density of gel cells and decreased the pore size compared to Az-C gel, indicating that P2k-dM constituted a structural component in the gel.

Az-C/PEG semi-IPN formation appears to be influenced by the molecular weight of the PEG. Az-C/P8k-dH solution was extremely viscous and hard to handle. The high viscosity limited homogeneous mixing of polymers and efficient formation of semi-IPN, as reflected by large variation in G' values of Az-C/P8k-dH gel. Cryo-SEM images support this speculation. Compared to Az-C/P2k-dM, Az-C/P6k-dH showed a relatively broad distribution of pore sizes, with some pores as large as those of Az-C and others similar to those of Az-C/P2k-dM. This reflects the effect of the relatively high molecular weight and limited mobility of P6k-dH on the mixing of two polymers.

The end group of the PEG was another influential factor in formation of semi-IPN. While incorporation of PEGs in Az-C increased G' and shortened the gelation time of the gel in most cases, Az-C/P2k-dH took longer ($43.7 \pm 2.0 \text{ s}$) to gel than Az-C ($38.5 \pm 1.5 \text{ s}$)

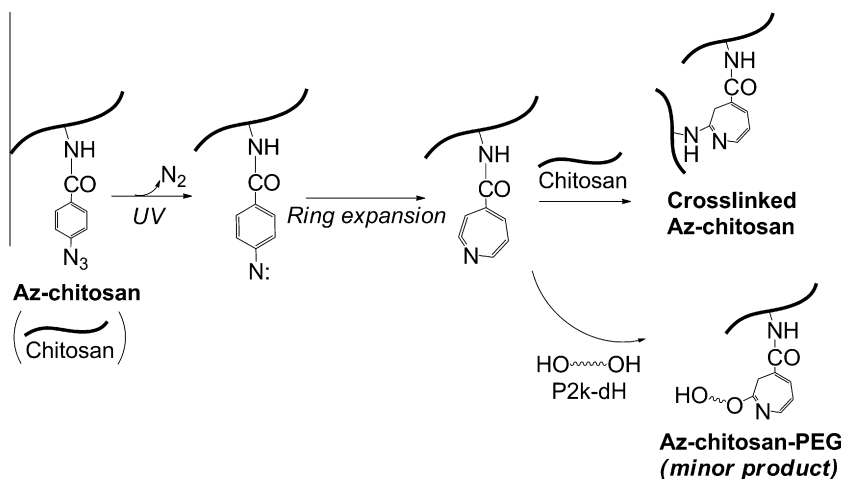
($p < 0.001$). We speculated that this difference might be due to the large number of reactive hydroxyl end groups of P2k-dH that could intercept the reactive nitrene and interfere with the covalent crosslinking of the Az-Cs. Although less nucleophilic than amine groups, hydroxyl groups can undergo a similar reaction as amines (Scheme 1). Since P2k-dH presented 2–4 times more hydroxyl groups (0.08 M) than the other PEGs (0.02–0.035 M) (Table 1), it had a greater chance of interfering with Az-C crosslinking. This hypothesis was supported by the fact that Az-C/P2k-dM (which has non-reactive methoxy groups instead of hydroxyl groups in both termini) had a much higher G' than Az-C/P2k-dH. P2k-dM was comparable to higher-molecular-weight PEGs in its effects on G' and gelation kinetics. In line with this observation, replacement of P4.6k-dH or P6k-dH with P5k-mM, which decreased the amount of hydroxyl groups to a smaller extent (from 0.035 M or 0.027 M to 0.016 M), did not significantly alter G' . Considering the effects of molecular weight and terminal groups of PEG on the semi-IPN formation, P2k-dM was considered the most desirable of the PEGs tested. The relatively low molecular weight of P2k-dM makes it easy to blend with Az-C, and it does not have hydroxyl termini to impede Az-C crosslinking.

A series of ex vivo and in vitro experiments were performed to test biocompatibility of Az-C/PEG gels. Although the ultimate biocompatibility testing for Az-C/PEG gels should be performed on damaged nerves in vivo, we attempted to approximate this scenario using nerve apposition and bioadhesive application ex vivo. We anticipated that the addition of PEG would not affect the biological effects of the gel in an adverse manner, due to the well-established safety profile of PEG [46]. The pore size decreased with the addition of PEG (Fig. 3), but it was not considered an issue because the gel was envisioned to be a support surrounding the injured nerves rather than a tissue scaffold. As expected, Az-C/PEG gels were found to be compatible with nerve cells and tissues, similar to Az-C [22]. First of all, Az-C/PEG gels had no effects on electrophysiological signal conduction through nerves ex vivo, similar to Az-C [22]. The lack of an observed response in CAP amplitude or latency to adhesive exposure does not indicate that Az-C will not impair conduction or healing, though it does suggest that Az-C is not acutely toxic to nerve function. Moreover, PC-12 cells grown with Az-C/PEG gels were no different from those on TCPS in the LDH release – an indicator of cell death [47]. For all surfaces, LDH release significantly decreased over time. Such behavior could be explained by some cells being initially non-adherent or only loosely attached to the surface and removed during the repeated medium changes. If non-adherent cells, which are more prone to rupture, were removed in the earlier phases of the

experiment, adherent cells, with a greater chance of survival, would be selected toward the later time points, resulting in a relatively low LDH level. Similar to our observation, Charlier et al. reported decreases in LDH activity with the culture conditions that encouraged PC-12 cell adhesion [48]. On the other hand, PC-12 cells appeared less proliferative on Az-C/PEGs than on TCPS on day 7 ($p < 0.001$) according to WST-1 assay. The lower cell viability on day 7 is, however, likely attributable to the lack of cell adhesion on Az-C/PEGs rather than the direct toxic effect of the gel components. Previously Az-C did not show toxicity at any of the time points tested (1, 4 and 7 days) [22], and PEG is commonly used to prevent cell adhesion on a surface [49,50]. The reduced cell adhesion to Az-C/PEG gels may have beneficial effects when used for nerve anastomosis and regeneration, as it can limit unwanted outgrowth of neural cells outside the anastomotic site.

The mean process length for cells growing on TCPS increased with time, extending neurites to 64 μm over 7 days, whereas cells growing on the Az-C/PEG gels extended processes whose lengths plateaued around 40 μm . This difference can be explained in at least two ways: first, PC-12 cells tend to extend longer neurites on rigid substrates like TCPS [51] than on soft hydrogel surfaces; and second, unlike those on flat TCPS surface, cells may have grown into Az-C/PEG gels spanning multiple focal depths. Optical microscopy may have underestimated the length of a neurite due to the lack of focus toward its end.

While PEG was primarily proposed to improve the mechanical properties of the Az-C gel, it may also be beneficial for nerve repair [28,29,52–55]. PEG is known to fuse cell membranes swiftly [27–29] and thus restore conduction in damaged axons within minutes in experimental settings [54–56]. Therefore, it is possible that PEG treatment may provide additional benefit through membrane fusion that could contribute to the overall functional recovery of nerves [54–58]. From the Az-C/P2k-dM gel, P2k-dM was released over 25 days by diffusion, showing that the gel served as a controlled delivery system of P2k-dM. The release pattern of Az-C/P2k-dM is desirable for nerve repair, because the initial burst release can provide a primary dose of PEG to assist in functional recovery of the primary nerve damage, while the remainder continues to reinforce the network. PEG slowly released thereafter would be helpful for healing of the secondary neural injury, as membrane damage can continue for 20 days [57]. PEG release may be faster in vivo, where chitosan is degraded by lysozyme [26]; however, the degradation should be slow enough to maintain PEG and gel for at least a week [59]. The released PEG is expected to be removed by renal filtration and biliary excretion [46].



Scheme 1. Potential mechanism of Az-C crosslinking and the interference of P2k-dH in the Az-C crosslinking.

5. Conclusions

PEG was blended with an Az-C photocrosslinkable hydrogel to improve the mechanical properties of Az-C as a nerve adhesive. The composite gels of PEG and Az-C had higher storage moduli and shorter gelation times than an Az-C gel or fibrin glue, and nerves anastomosed with an Az-C/PEG gel tolerated a higher force than those with fibrin glue prior to failure. These effects are likely due to the formation of a semi-IPN network, where PEG interpenetrates the covalent Az-C network and physically reinforces the network. Cryo-SEM demonstrated the participation of PEG in the Az-C/PEG gel network. The cryo-SEM and rheological measurements suggest that low-molecular-weight PEG with a non-reactive terminal group would be most desirable for the efficient formation of a semi-IPN with Az-C. A series of ex vivo and in vitro cell experiments indicate that Az-C/PEG gels are compatible with nerve tissues and cells. Given the membrane-fusing potential of PEG, the ability of the Az-C/PEG gels to release PEG over a prolonged period may provide an additional benefit to nerve repair by maintaining nerve membrane integrity and subsequently cellular survival.

Acknowledgements

The authors thank Prof. Xinqiao Jia (University of Delaware) for insightful advice and suggestions for the PEG effect, Prof. Gudrun Schmidt for help with rheological testing, Prof. David Thompson and Dr. Seok-Hee Hyun for help with GPC, and Ms. Debra Sherman for help with the cryo-SEM. This study was funded by the Showalter Trust Award (R.S.) and the Indiana Spinal Cord and Brain Injury Fund (R.S.). This work was also supported in part by a grant from the Lilly Endowment, Inc. to College of Pharmacy, Purdue University (Y.Y.). The authors also wish to acknowledge the financial support of the Indiana Clinical and Translational Sciences Institute-PDT (PHS NCCR Grant No. 5TL1RR025759-02) (R.S., T.R.) and the Winifred Beatrice Bilsland Endowment (T.R., Z.A.).

Appendix A. Supplementary data

Supplementary data associated with this article can be found, in the online version, at [doi:10.1016/j.actbio.2012.01.022](https://doi.org/10.1016/j.actbio.2012.01.022).

References

- [1] Colohan AR, Pitts LH, Rosegay H. Injury to the peripheral nerves. Stamford, CT: Appleton & Lange; 1996.
- [2] Grant GA, Goodkin R, Kliot M. Evaluation and surgical management of peripheral nerve problems. *Neurosurgery* 1999;44:825–39.
- [3] Kallio PK, Vastamaki M, Solonen KA. The results of secondary microsurgical repair of radial nerve in 33 patients. *J Hand Surg Br* 1993;18:320–2.
- [4] Vastamaki M, Kallio PK, Solonen KA. The results of secondary microsurgical repair of ulnar nerve injury. *J Hand Surg Br* 1993;18:323–6.
- [5] Kallio PK, Vastamaki M. An analysis of the results of late reconstruction of 132 median nerves. *J Hand Surg Br* 1993;18:97–105.
- [6] Lee SK, Wolfe SW. Peripheral nerve injury and repair. *J Am Acad Orthop Surg* 2000;8:243–52.
- [7] Lundborg G. A 25-year perspective of peripheral nerve surgery: evolving neuroscientific concepts and clinical significance. *J Hand Surg-Am* 2000;25A:391–414.
- [8] DeLee JC, Smith MT, Green DP. The reaction of nerve tissue to various suture materials: a study in rabbits. *J Hand Surg Am* 1977;2:38–43.
- [9] Isaacs J, Klumb I, McDaniel C. Preliminary investigation of a polyethylene glycol hydrogel “nerve glue”. *J Brachial Plex Peripher Nerve Inj* 2009;4:16.
- [10] Johnson TS, O’Neill AC, Motarjem PM, Amann C, Nguyen T, Randolph MA, et al. Photochemical tissue bonding: a promising technique for peripheral nerve repair. *J Surg Res* 2007;143:224–9.
- [11] Narakas A. The use of fibrin glue in repair of peripheral-nerves. *Orthop Clin North Am* 1988;19:187–99.
- [12] Martins RS, Siqueira MG, da Silva CF, de Godoy BO, Plese JPP. Electrophysiologic assessment of regeneration in rat sciatic nerve repair using suture, fibrin glue or a combination of both techniques. *Arq Neuro-Psiquiatr* 2005;63:601–4.
- [13] Bento RF, Miniti A. Anastomosis of the intratemporal facial nerve using fibrin tissue adhesive. *Ear Nose Throat J* 1993;72:663–72.
- [14] Martins RS, Siqueira MG, Da Silva CF, Plese JPP. Overall assessment of regeneration in peripheral nerve lesion repair using fibrin glue, suture, or a combination of the 2 techniques in a rat model. Which is the ideal choice? *Surg Neurol* 2005;64:S10–6.
- [15] Menovsky T, Beek JF. Laser, fibrin glue, or suture repair of peripheral nerves: a comparative functional, histological, and morphometric study in the rat sciatic nerve. *J Neurosurg* 2001;95:694–9.
- [16] Feldman MD, Sataloff RT, Epstein G, Ballas SK. Autologous fibrin tissue adhesive for peripheral-nerve anastomosis. *Arch Otolaryngol Head Neck Surg* 1987;113:963–7.
- [17] Smahel J, Meyer VE, Bachem U. Glueing of peripheral nerves with fibrin experimental studies. *J Reconstr Microsurg* 1987;3:211–8.
- [18] Sames M, Blahos J, Rokyta R, Benes V. Comparison of microsurgical suture with fibrin glue connection of the sciatic nerve in rabbits. *Physiol Res* 1997;46:303–6.
- [19] Goldman M. Transmission of symptomatic parvovirus B19 infection by fibrin sealant used during surgery: M. Hino, O. Ishiko, K. Honda, et al. *Br J Haematol* 108:194–195, 2000. *Transfus Med Rev* 2000;14:379–80.
- [20] Frenkel SR, Di Cesare PE. Scaffolds for articular cartilage repair. *Ann Biomed Eng* 2004;32:26–34.
- [21] Yeo Y, Geng W, Ito T, Kohane DS, Burdick J, Radisic M. A photocrosslinkable hydrogel for myocyte cell culture and injection. *J Biomed Mater Res* 2006;81B:312–22.
- [22] Rickett T, Amoozgar Z, Tuckek CA, Park J, Yeo Y, Shi R. A rapidly photocrosslinkable chitosan hydrogel for peripheral neurosurgeries. *Biomacromolecules* 2011;12:57–65.
- [23] Rickett T, Amoozgar Z, Sun WJ, Yeo Y, Shi RY. A photo-crosslinkable chitosan hydrogel for peripheral nerve anastomosis. In: Shi R, Fu WJ, Wang YQ, Wang HB, editor. Proceedings of the 2009 2nd international conference on biomedical engineering and informatics, vols. 1–4. New York: IEEE; 2009. pp. 1078–82.
- [24] Ono K, Saito Y, Yura H, Ishikawa K, Kurita A, Akaike T, et al. Photocrosslinkable chitosan as a biological adhesive. *J Biomed Mater Res* 2000;49:289–95.
- [25] Prasitsilp M, Jenwithisuk R, Kongsuwan K, Damrongchai N, Watts P. Cellular responses to chitosan in vitro: the importance of deacetylation. *J Mater Sci Mater Med* 2000;11:773–8.
- [26] Muzzarelli RAA. Biochemical significance of exogenous chitins and chitosans in animals and patients. *Carbohydr Polym* 1993;20:7–16.
- [27] Lentz BR. Polymer-induced membrane-fusion – potential mechanism and relation to cell-fusion events. *Chem Phys Lipids* 1994;73:91–106.
- [28] Shi R, Borgens RB. Anatomical repair of nerve membranes in crushed mammalian spinal cord with polyethylene glycol. *J Neurocytol* 2000;29:633–43.
- [29] Shi R, Blight AR, Borgens RB. Functional reconnection of severed mammalian spinal cord axons by a molecular surfactant. *J Neurotrauma* 1999;16:727–38.
- [30] Serrero AI, Trombotto Sp, Bayon Y, Gravagna P, Montanari S, David L. Polysaccharide-based adhesive for biomedical applications: correlation between rheological behavior and adhesion. *Biomacromolecules* 2011;12:1556–66.
- [31] Phillips JB, Smit X, De Zoysa N, Afoke A, Brown RA. Peripheral nerves in the rat exhibit localized heterogeneity of tensile properties during limb movement. *J Physiol* 2004;557:879–87.
- [32] Rickett T, Li JM, Patel M, Sun WJ, Leung G, Shi RY. Ethyl-cyanoacrylate is acutely nontoxic and provides sufficient bond strength for anastomosis of peripheral nerves. *J Biomed Mater Res A* 2009;90A:750–4.
- [33] Chaplan SR, Guo HQ, Lee DH, Luo L, Liu CL, Kuei C, et al. Neuronal hyperpolarization-activated pacemaker channels drive neuropathic pain. *J Neurosci* 2003;23:1169–78.
- [34] Narahashi T, Moore JW, Scott WR. Tetrodotoxin blockage of sodium conductance increase in lobster giant axons. *J Gen Physiol* 1964;47:965–74.
- [35] Shi R, Luo J, Peasley M. Acrolein inflicts axonal membrane disruption and conduction loss in isolated guinea-pig spinal cord. *Neuroscience* 2002;115:337–40.
- [36] Greene LA, Tischler AS. Establishment of a noradrenergic clonal line of rat adrenal pheochromocytoma cells which respond to nerve growth factor. *Proc Natl Acad Sci USA* 1976;73:2424–8.
- [37] Siepmann J, Peppas NA. Modeling of drug release from delivery systems based on hydroxypropyl methylcellulose (HPMC). *Adv Drug Deliv Rev* 2001;48:139–57.
- [38] Temple CLF, Ross DC, Dunning CE, Johnson JA, King GJW. Tensile strength of healing peripheral nerves. *J Reconstr Microsurg* 2003;19:483–8.
- [39] Nishimura MT, Mazzer N, Barbieri CH, Moro CA. Mechanical resistance of peripheral nerve repair with biological glue and with conventional suture at different postoperative times. *J Reconstr Microsurg* 2008;24:327–32.
- [40] Cho CS, Han SY, Ha HJ, Kim SH, Lim DY. Clonazepam release from bioerodible hydrogels based on semi-interpenetrating polymer networks composed of poly(epsilon-caprolactone) and poly(ethylene glycol) macromer. *Intl J Pharm* 1999;181:235–40.
- [41] Mandal BB, Kapoor S, Kundu SC. Silk fibroin/polyacrylamide semi-interpenetrating network hydrogels for controlled drug release. *Biomaterials* 2009;30:2826–36.
- [42] Dinu MV, Perju MM, Drăgan ES. Porous semi-interpenetrating hydrogel networks based on dextran and polyacrylamide with superfast responsiveness. *Macromol Chem Phys* 2011;212:240–51.

- [43] Muniz EC, Geuskens G. Compressive elastic modulus of polyacrylamide hydrogels and semi-IPNs with poly(N-isopropylacrylamide). *Macromolecules* 2001;34:4480–4.
- [44] Kayaman-Apohan N, Baysal BM. Semi-interpenetrating hydrogel networks of poly(2-hydroxyethyl methacrylate) with poly[(D, L-lactic acid)-co-(ϵ -caprolactam)]. *Macromol Chem Phys* 2001;202:1182–8.
- [45] Rokhade AP, Agnihotri SA, Patil SA, Mallikarjuna NN, Kulkarni PV, Aminabhavi TM. Semi-interpenetrating polymer network microspheres of gelatin and sodium carboxymethyl cellulose for controlled release of ketorolac tromethamine. *Carbohydr Polym* 2006;65:243–52.
- [46] Webster R, Didier E, Harris P, Siegel N, Stadler J, Tilbury L, et al. PEGylated proteins: evaluation of their safety in the absence of definitive metabolism studies. *Drug Metab Dispos* 2007;35:9–16.
- [47] Legrand C, Bour JM, Jacob C, Capiamont J, Martial A, Marc A, et al. Lactate dehydrogenase (LDH) activity of the cultured eukaryotic cells as marker of the number of dead cells in the medium [corrected]. *J Biotechnol* 1992;25:231–43.
- [48] Charlier N, Leclere N, Felderhoff U, Heldt J, Kietzmann T, Obladen M, et al. Hypoxia-induced cell death and changes in hypoxia-inducible factor-1 activity in PC12 cells upon exposure to nerve growth factor. *Mol Brain Res* 2002;104:21–30.
- [49] Boulmedais F, Frisch B, Etienne O, Lavalle P, Picart C, Ogier J, et al. Polyelectrolyte multilayer films with pegylated polypeptides as a new type of anti-microbial protection for biomaterials. *Biomaterials* 2004;25:2003–11.
- [50] Chen Y, Kang ET, Neoh KG, Wang P, Tan KL. Surface modification of polyaniline film by grafting of poly(ethylene glycol) for reduction in protein adsorption and platelet adhesion. *Synth Met* 2000;110:47–55.
- [51] Leach JB, Brown XQ, Jacot JG, DiMilla PA, Wong JY. Neurite outgrowth and branching of PC12 cells on very soft substrates sharply decreases below a threshold of substrate rigidity. *J Neural Eng* 2007;4:26–34.
- [52] Ditor DS, John SM, Roy J, Marx JC, Kittner C, Weaver LC. Effects of polyethylene glycol and magnesium sulfate administration on clinically relevant neurological outcomes after spinal cord injury in the rat. *J Neurosci Res* 2007;85:1458–67.
- [53] Koob AO, Borgens RB. Polyethylene glycol treatment after traumatic brain injury reduces β -amyloid precursor protein accumulation in degenerating axons. *J Neurosci Res* 2006;83:1558–63.
- [54] Shi R, Borgens RB. Acute repair of crushed guinea pig spinal cord by polyethylene glycol. *J Neurophysiol* 1999;81:2406–14.
- [55] Donaldson J, Shi R, Borgens R. Polyethylene glycol rapidly restores physiological functions in damaged sciatic nerves of guinea pigs. *Neurosurgery* 2002;50:147–57.
- [56] Britt JM, Kane JR, Spaeth CS, Zuzek A, Robinson GL, Gbanaglo MY, et al. Polyethylene glycol rapidly restores axonal integrity and improves the rate of motor behavior recovery after sciatic nerve crush injury. *J Neurophysiol* 2010;104:695–703.
- [57] Shi RY. The dynamics of axolemmal disruption in guinea pig spinal cord following compression. *J Neurocytol* 2004;33:203–11.
- [58] Borgens RB, Shi R. Immediate recovery from spinal cord injury through molecular repair of nerve membranes with polyethylene glycol. *FASEB J* 2000;14:27–35.
- [59] Obara K, Ishihara M, Ishizuka T, Fujita M, Ozeki Y, Maehara T, et al. Photocrosslinkable chitosan hydrogel containing fibroblast growth factor-2 stimulates wound healing in healing-impaired db/db mice. *Biomaterials* 2003;24:3437–44.